

QTM: A Software Package for the Analysis of QCM-Data

0 Preface	2
1 Overall Organization	3
2 Background.....	4
2.1 <i>The small load approximation (SLA)</i>	4
2.2 <i>Short-comings of the SLA, perturbation analysis</i>	4
2.3 <i>Gravimetric sensing</i>	5
2.4 <i>Semi-infinite viscoelastic media, measurements of viscosity</i>	5
2.5 <i>Viscoelastic layer systems, the acoustic multilayer formalism (AMF)</i>	6
2.6 <i>Roughness</i>	6
2.7 <i>Elastic loading across point contacts</i>	7
2.8 <i>Coupled resonances</i>	7
2.9 <i>Effects not covered by QTM</i>	7
3 A Tour Through QTM.....	7
3.1 <i>Inspecting data and model parameters in the Main Form</i>	7
3.2 <i>Fitting</i>	8
3.3 <i>Analyze entire files</i>	9
3.4 <i>Chi² landscape</i>	10
3.5 <i>Further parameters entering the analysis</i>	10
4 Some Details of the Machinery	11
4.1 <i>Thickness versus mass per unit area</i>	11
4.2 <i>Representation of viscoelasticity</i>	11
4.3 <i>Reference state</i>	12
4.4 <i>Discard data from the fundamental</i>	12
4.5 <i>Film resonances</i>	12
4.6 <i>Electrode effects</i>	13
4.7 <i>Viscoelastic profiles</i>	13
5 Underlying Equations	13
5.1 <i>Layer systems</i>	13
5.2 <i>Roughness</i>	14
5.3 <i>Elastic loading across point contacts</i>	15
5.4 <i>Coupled resonances</i>	15
5.5 <i>Perturbation analysis</i>	18
5.5.1 <i>Semi-infinite liquid (can be a viscoelastic medium)</i>	18
5.5.2 <i>Viscoelastic film in air</i>	18
5.5.3 <i>Viscoelastic film in liquid</i>	19
5.5.4 <i>Two viscoelastic films in air</i>	19
5.5.5 <i>Two viscoelastic films in a liquid</i>	20
6 Glossary	22
7 References	23

0 Preface

QTM implements various algorithms for the analysis of shifts of frequency and bandwidth ($\Delta f(n)$ and $\Delta \Gamma(n)$ with n the overtone order) acquired with a quartz crystal microbalance (QCM). QTM has grown in a research environment and keeps evolving. In that process, oddities and bugs appear. Please give feedback.

Introductions to the background – written by myself^a – can be found in references 1, 2, and 3. For reviews on the QCM in general see, for instance, Refs. 4, 5, 6, 7, and 8.

I have recently removed some options, which made QTM look complicated and which I myself rarely used. Realistically, there are some artifacts in the operation of the QCM (resulting from crystal defects, static stress, coupling to anharmonic sidebands, etc.), which at present cannot be accounted for in the modeling process. Given these systematic uncertainties, a robust analysis usually is a simple analysis. One can construct elaborate models and calculate Δf and $\Delta \Gamma$ from the system parameters, but the machine does not run backwards: Experimental values of Δf and $\Delta \Gamma$ will not allow to differentiate between two such complicated models. Following these considerations, I removed the section on continuous viscoelastic profiles (which might be used to reproduce the behavior of polymer brushes). I also removed the option to employ user-specified dispersion laws (user-specified relations for $G'(\omega)$ and $G''(\omega)$). QTM now only allows for power laws (Eq. 7). Also, QTM now allows for a maximum of two layers (down from four in the previous version). There is no module accounting for piezoelectric stiffening. Again: This is not to say that the more advanced models were meaningless or wrong. It only is meant to say that the comparison to experiment is difficult.

Notation: The shifts of frequency and half bandwidth are called Δf and $\Delta \Gamma$. Dissipative processes are quantified by the half-bandwidth, here. Γ is related to the “dissipation factor” by the relation $D = Q^{-1} = 2\Gamma/f_r$. Δf and $\Delta \Gamma$ can be collected in a complex frequency shift $\tilde{\Delta f} = \Delta f + i\Delta \Gamma$. (The tilde denotes a complex variable.) Δf looks like “Df” in QTM, $\Delta \Gamma$ looks like “DG”. For further definitions of variables, see the glossary in section 6.

“Experimental data” in QTM are shifts of resonance frequency and bandwidth. Whether these have been obtained with impedance analysis or ring-down, makes no difference to QTM.

Here is an empathetic remark from Numerical Recipes [Ref. 13, on-line versions exist] directed at those, who look before they leap (who first fiddle around with the parameters to get a feel for the situation, before they click the Fit-button): “Unfortunately, many practitioners ... deem a fit acceptable if a graph of the data and model “looks good”. This approach is known as *chi-by-eye*. Luckily, these practitioners get what they deserve”. Alright! As for me, I keep looking before I leap.

QTM is freeware.^b When results obtained with QTM are mentioned in publications, its use should be acknowledged.

In developing QTM I have profited from interactions with numerous people. I would like to specifically mention Ilya Reviakine, Ralf Richter, and Arne Langhoff.

Clausthal, Dec 2017

Diethelm Johannsmann

^a References to the previous work are contained in these overviews. Not being scientific literature in the narrow sense, this manual is short on quotes.

^b Being an executable file, QTM.exe often gets stuck in firewalls. Send it via Cryptshare or similar software.

1 Overall Organization

To get started, save all files associated to QTM into a folder of your choice. There is no installer. Click QTM.exe to launch QTM. On start-up, QTM reads-in a certain status (file names of previous projects, size and position of Main Form, etc.) from the file QTM.ini.

QTM saves work in files with the extensions .qtm and .qtd. While you work, QTM saves all steps into TmpQTM.qtm (and TmpQTM.qtd in case you analyze entire files). This information is transferred to the file of your choice once you save. *.qtm contains choices and options as well experimental data, fitted values, and fit parameters for one single data set. *.qtd contains data, fitted values, and fitted parameters for many data sets. *.qtm and *.qtd are ASCII files. *.qtm has the structure of an initialization file. *.qtm can be opened with an editor; one can guess the meanings of the variables to some extent.

Experimental data can be edited into the table on the left-hand side in the Main Form. They can also be imported from the clipboard with the button <- Clipboard. One would typically collect the data – in the format shown in the QTM Main Form – in Excel, load this set into the clipboard with ControlA, and then click <- Clipboard in QTM. There is a similar table for importing entire files in the Form Analyze Entire Files. Note: In the latter case, the data in the clipboard need to be organized in lines, whereas they need to be organized as two columns for import into the Main Form. Data can be

The screenshot shows the QTM software interface with the following components:

- File Menu:** File, Model, Show, Graphs, Limits, Parameters, Reference, χ^2 -Landscape, Analyze Entire Files, About.
- Parameter Settings:**
 - Thickness [nm]: 2.512
 - ρ [g/cm³]: 1.000
 - $J'(f_{ref})$ [MPa⁻¹]: 1.34541
 - PL.Exp. J' : -1.030
 - $J''(f_{ref})$ [MPa⁻¹]: 1.39886
 - PL.Exp. J'' : -0.254
 - Fit-Pars -> Clipboard: J', J''
 - ρ [g/cm³]: 1.000
 - $\eta'(f_{ref})$ [mPas]: 0.89000
 - PL.Exp. η' : 0.002
 - $\eta''(f_{ref})$ [mPas]: 0.00000
 - PL.Exp. η'' : 0.000
 - Fit-Pars -> Clipboard: η', η''
- Model Fit Table:**

Model	Fit
x 10	/ 10
x 5	/ 5
x 2	/ 2
x 1.5	/ 1.5
x 1.1	/ 1.1
x 1.01	/ 1.01
- Experimental Data Table:**

n	Df/n [Hz]	DD [10 ⁻⁶]
1.0	-14.05	0.00
3.0	-12.59	1.00
5.0	-11.10	1.20
7.0	-10.22	1.30
9.0	-9.75	1.34
11.0	-9.47	1.25
13.0	-9.49	1.24
- Graphs:**
 - Top Graph: Df [Hz] vs Overtone Order n. Shows experimental data points (open circles) and a fitted curve (red line) for the Acoustic Multilayer Formalism.
 - Bottom Graph: DG [Hz] vs Overtone Order n. Shows experimental data points (open circles) and a fitted curve (red line) for the Acoustic Multilayer Formalism.
- Status Bar:**
 - Fundamental : 5.000 MHz
 - Ref. Freq. VE Pars : 30.000 MHz
 - Z_q [10⁻⁶]: 8.80 kg/(m² s)
 - AMF, Fresnel-Type
 - Ref: t_e : 0.0

imported into the Form *Analyze Entire Files* from a text-file, as well. Such text files might be produced by QTools. The file named *template_for_input.txt* contains an example showing the proper format.

Experimental data for input may be expressed as either sets of values $\{\Delta f, \Delta\Gamma\}$ or sets of $\{\Delta f/n, \Delta D\}$.^c The term “set” pertains to data for the different overtones at one single time.

Note: “*F*” in QTools is the *overtone-normalized* frequency shift. “*F*” is $\Delta f/n$. There is a box to choose between $\{Df[\text{Hz}], DG[\text{Hz}]\}$ and $\{Df/n[\text{Hz}], DD[10^{-6}]\}$ in both forms.

Results can be exported in different ways:

- The button *Fits -> Clipboard* saves data and fitted data to the clipboard.
- The button *Fit-Pars -> Clipboard* saves the fit parameters to the clipboard.
- The buttons *Graph -> Clipboard* save the respective graph to the clipboard.

Most of the time, the user tries to find model parameters, which make the model (predictions shown as a red line the Main Form) agree with experimental data. It is strongly advised to not jump to a fit right away, but to rather play around with parameters by hand and see, what a meaningful set of parameters might be. In order to do that, make a certain parameter “active” by checking the *round* button next to it. Once a parameters is active, it can be increased or decreased with the buttons “×5”, “/5” etc. on the left-hand side of the Main Form. Parameters can also be edited into the respective field. For further information on the Main Form, see section 3.1

2 Background

2.1 The small load approximation (SLA)

The overarching concept in the modeling of QCM results is the small-load approximation. The small load approximation (SLA) states that the complex frequency shift is proportional to the ratio of stress and velocity at the resonator surface, where both stress and velocity are complex amplitudes. Since the SLA is a linear relation, it can be averaged over the area of the resonator. More quantitatively, the SLA is expressed as

$$\frac{\Delta \tilde{f}}{f_0} \approx \frac{i}{\pi Z_q} \tilde{Z}_L = \frac{i}{\pi Z_q} \frac{\langle \hat{\sigma}_{\parallel} \rangle_{area}}{\hat{v}} \quad \text{Eq. 1}$$

\tilde{Z}_L is the “load impedance”, which is ratio of the area-averaged stress to the tangential velocity. See the glossary in section 6 for the meaning of the other variables. There are extensions of the SLA covering dielectric effects (Chapter 5 in [3]) and non-tangential stress (Chapter 6.1 in [3]). These are not part of QTM.

2.2 Short-comings of the SLA, perturbation analysis

The SLA does *not* cover the effects originating from flexural contributions (Chapter 6.1.3 in [3]).

The SLA produces noticeably incorrect results when applied to thin films in air or vacuum. These are caused by the linearization inherent to the SLA. These short-comings have nothing to do with flexural contributions. They occur within the parallel plate model. The solution to this problem is to demand $\tilde{Z}_{mot} = 0$ with \tilde{Z}_{mot} given in Eq. 4.5.9 in [3]. One can numerically search for values of Δf and $\Delta\Gamma$ leading to $\tilde{Z}_{mot} = 0$. A previous version of QTM implemented this algorithm. One may also find approximate values for Δf and $\Delta\Gamma$ by an iterative “perturbation approach” (Chapter 6.2 in [3]) and

^c An opinion on terminology: „Dissipation“ in science usually denotes a process by which non-thermal energy is converted to thermal energy. Calling the inverse Q-factor “dissipation” is unorthodox.

section 5.5 below). “Approximate” in this context implies that the results from the 3rd-order and the 5th-order perturbation calculations are more accurate than the results obtained with the SLA *in the thin film limit*. The perturbation calculation does not capture the film resonance (section 4.5). In order to capture the film resonance and – at the same time – avoid the errors resulting from linearization, one has to numerically solve $\tilde{Z}_{mot} = 0$ for Δf and $\Delta\Gamma$. One needs to keep in mind, though, that \tilde{Z}_{mot} is calculated within the parallel plate model. Solving $\tilde{Z}_{mot} = 0$ for Δf and $\Delta\Gamma$ is by no means the ultimate answer to the modeling challenge.

The differences between results obtained with the perturbation approach and results obtained with the SLA are most noticeable for films in air.

2.3 Gravimetric sensing

If the sample is rigid, it only affects the resonance frequency through its inertia. Examples for rigid samples are films with a thickness much below the wavelength of sound. Tightly adsorbed nanoparticles can also be inertial loads. For inertial loads, the Sauerbrey equation applies:

$$\frac{\Delta f}{f_0} \approx -n \frac{m_f}{m_q} \quad \text{Eq. 2}$$

The Sauerbrey relation is sometimes memorized as $\Delta f/f = -m_f/m_q$ (with $f = nf_0$). The Sauerbrey equation is often inverted, so that the mass per unit area is on the left-hand side:

$$m_f = -\frac{Z_q}{2f_0^2} \frac{\Delta f}{n} = -\frac{\sqrt{\rho_q G_q}}{2f_0^2} \frac{\Delta f}{n} = -C \frac{\Delta f}{n} \quad \text{Eq. 3}$$

C is the mass-sensitivity constant. Its value is 17.7 ng cm⁻² Hz⁻¹ for 5-MHz resonators. Using the Sauerbrey equation, any frequency shift can be straight-forwardly converted to an equivalent change in mass per unit area. The Sauerbrey equation is explicit. A change of 5.6 Hz in $-\Delta f/n$ corresponds to 1 nm in film thickness, if the density is 1 g/cm³ (assuming $f_0 = 5$ MHz). QTM recovers the Sauerbrey limit for thin, stiff films. Again, QTM is not needed for the analysis of experiments in terms of gravimetry. One may directly convert from $-\Delta f/n$ to mass per unit area.

2.4 Semi-infinite viscoelastic media, measurements of viscosity

For semi-infinite media, the viscosity-density product follows from the Gordon-Kanazawa-Mason relation (Eq. 4 and Eq. 5). For semi-infinite media (such as a bulk liquid), the load impedance is the same as the acoustic shear-wave impedance of the medium. The latter is $(\rho_{liq} \tilde{G}_{liq})^{1/2} = (\rho_{liq} i \omega \tilde{\eta}_{liq})^{1/2}$. The index liq here denotes the bulk medium (which may be may not be a Newtonian liquid). More quantitatively, one has

$$\frac{\Delta f}{f_0} = \frac{-1+i}{\sqrt{2}\pi Z_q} \sqrt{\rho_{liq} \omega (\eta_{liq}' - i \eta_{liq}'')} = \frac{i}{\pi Z_q} \sqrt{\rho_{liq} (G_{liq}' + i G_{liq}'')} \quad \text{Eq. 4}$$

This equation can be inverted, such that the product of the shear modulus and the density (or the viscosity-density product) is on the left-hand side:

$$\rho_{liq} \tilde{G}_{liq} = -\left(\pi Z_q \frac{\Delta f}{f_0}\right)^2, \quad \rho_{liq} \tilde{\eta}_{liq} = -\frac{1}{i\omega} \left(\pi Z_q \frac{\Delta f}{f_0}\right)^2, \quad \text{Eq. 5}$$

Eq. 5 also is explicit. QTM is not needed for the analysis of experiments in which the QCM probes a viscosity.

Note: The left-hand side in Eq. 5 contains the product of ρ_{liq} and \tilde{G}_{liq} (or ρ_{liq} and $\tilde{\eta}_{liq}$). The two parameters cannot be determined separately. Stated differently, the QCM determines the viscosity-density-product, not the viscosity alone.

2.5 Viscoelastic layer systems, the acoustic multilayer formalism (AMF)

There is a time-honored formalism to calculate the periodic stress at a resonators surface caused by planar layer systems. The author calls this calculation the “acoustic multilayer formalism” (AMF). The formalism is adapted from an analogous set of equation in optics, where the latter carries the name Fresnel formalism. Each layer supports two plane waves (propagating upwards and downwards), the amplitudes of which are fixed by the boundary conditions. For up to two layers, the results can actually be expressed in analytical form and fit into one line (section 5.1). What is sometimes called “Voigt model”, is equivalent to the AMF.^d

2.6 Roughness

Roughness is a difficult topic. Practical samples often are slightly rough. Roughness certainly affects Δf and $\Delta \Gamma$. However, assumptions on the details of the geometry are needed to rigorously model roughness. (Such models *are* feasible, using finite element analysis.) QTM implements three equation sets (following Ref. 9), which were derived making assumptions on the geometry. There is “shallow roughness” meaning that, firstly, the vertical scale is smaller than the horizontal scale and that, secondly, the vertical scales is much less than the penetration depth of the shear wave, δ (and, also, that the roughness is Gaussian in a certain sense). The vertical scale and the horizontal scale are given by the parameters h_r and l_r . There are two different sets of equations, applicable to the cases $l_r \ll \delta$ (small-scale roughness, Eq. 15) and $l_r \gg \delta$ (large-scale roughness, and Eq. 16). QTM should bark when the user picks values for h_r and l_r outside the applicability of the respective equation set.

In addition to the model for shallow roughness, there is a model covering roughness using Darcy flow (Eq. 17). The rough surface is treated as a porous medium. The parameters of the model are L (the thickness of the rough layer) and ξ_H (ξ_H , the scale of roughness).

Roughness effects can be combined with viscoelastic layers. The rough interface then is assumed to be the interface between the last layer and the bulk liquid (Figure 2). Roughness effects as treated by QTM only exist, when the resonator is immersed in a bulk liquid. More technically, the shear-wave impedance of the liquid is replaced by what is called $Z_{liq,eff}$ in Eq. 15 – Eq. 17. Again: Result obtained with these equations should not be over-interpreted.

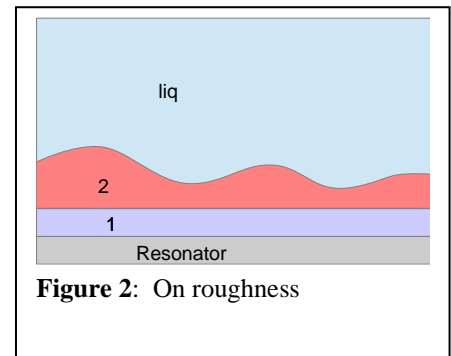


Figure 2: On roughness

^d The “Voigt-model” as currently used by QTools simply states that $\tilde{G}(\omega) = G'(\omega) + iG''(\omega)$. No statement is made on how, exactly, G' and G'' depend on ω . (There have been changes in this regard. Now, QTools also implements power laws.) That the complex shear modulus should contain a real and an imaginary part, is not usually viewed as the content of a “model”. In rheology, the Voigt model states that G' should be independent of ω and that G'' should scale as ω . That was also so in the very first form of the “Voigt-model” from QTools, but this approximation is not justified in most cases of practical relevance for the QCM. The Voigt model from rheology represents a medium as a spring and a dashpot mounted in parallel. The “Maxwell model” arranges the spring and the dashpot in series, which leads to a different prediction on the ω -dependence of \tilde{G} .

2.7 Elastic loading across point contacts

As first shown by Dybwad in 1985,¹⁰ the frequency may also *increase* when the resonator comes into contact with a sample. This happens with point contacts. These add little inertia to the system, but increase the resonator's overall stiffness. For a point contact between the resonator surface and a large external object (such as a sphere with a diameter of 100 μm and above) the contact stiffness can be explicitly obtained from the frequency shift (Eq. 18, section 11.3 in [3]). For the simple cases, there is no need for modeling with QTM. QTM implements elastic contacts, because the contacts stiffness might depend on frequency and because there may be offsets in Δf and $\Delta\Gamma$. For more details see section 5.3.

2.8 Coupled resonances

If particles touching the resonator are not heavy enough to be clamped in space by inertia, they turn into resonators of their own, where the restoring force is exerted by the contact (Figure 3). For more details see sections 11.4 and 11.5 in [3]). Coupled resonances are intriguing in many ways,¹¹ but turning this fascination into robust fit results has often been difficult. QTM tries anyway.

2.9 Effects not covered by QTM

The above list concerns models, which are simple enough to be translated into an algorithm. There are other sources of shifts in frequency and bandwidth, which are either too complicated or simply outside the scope. Below is a list of effects which are *not* covered by QTM.

- Energy trapping including the poorly predictable behavior of the fundamental.
- Compressional waves (section 7.6 in [3]).
- Temperature and static stress (section 17.2 in [3]).
- High amplitudes (nonlinear effects, section 13 in [3]).
- Structure on the scale of the wavelength of sound^e (section 12 in [3], Ref. 12).

3 A Tour Through QTM

3.1 Inspecting data and model parameters in the Main Form

The Main Form has already been covered to some extent in section 1. A few further comments:

- QTM has input verification. An input is only accepted after the user hits *Return*.
- Shifts of frequency and bandwidth are always to be understood as shifts with respect to some reference state (see also section 4.3). The reference state is edited in the *Reference Form*. The user may also turn some state into the reference state by clicking *-> Reference*.
- It is helpful to activate limits on the parameters in the *Limits Form*. QTM offers default limits, when the user clicks *Defaults* in the Limits Form. If limits are active, the respective fields in Main Form have light blue background. Otherwise, the background is white. If a certain parameter is at the

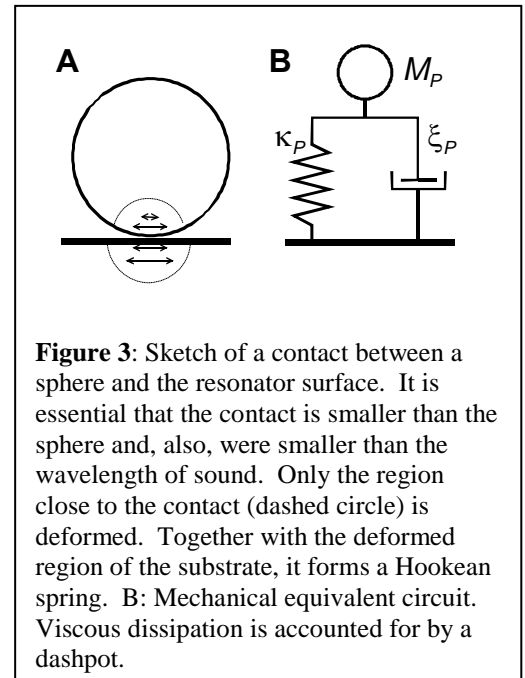


Figure 3: Sketch of a contact between a sphere and the resonator surface. It is essential that the contact is smaller than the sphere and, also, were smaller than the wavelength of sound. Only the region close to the contact (dashed circle) is deformed. Together with the deformed region of the substrate, it forms a Hookean spring. B: Mechanical equivalent circuit. Viscous dissipation is accounted for by a dashpot.

^e Roughness amounts to such structures. The models for roughness as proposed by the Tel-Aviv group make numerous assumptions. Generally speaking, predicting Δf and $\Delta\Gamma$ produced by arbitrary structures is a challenge with significant recent success.[12]

limit or beyond the limit, the number turns red.

Some limits are rigorous. For instance, thicknesses and moduli must never be negative. There also are strict limits for the power-law exponents (Eq. 7). In other cases (such as the maximum reasonable thickness of a layer), the limits are a matter of personal judgement. If the fit tries to make a layer very soft, it runs into an instability because the term kd in $\tan(kd)$ then becomes large. $\tan(kd)$ occurs often. One should make the lower limits of the moduli slightly larger than zero for that reason.

Watch out: *When limits are imposed, the simplex algorithm sometimes increases χ^2 .* The limits intervene into the simplex algorithm to the extent, that it may stop where it should not stop. Keep a close eye on the value of χ^2 .

- The Form *Graphics* allows to set titles and subtitles of the graphs.
- For the representation of viscoelastic parameters see section 4.2.
- Most users are interested viscoelastic layer systems, to be modeled with the acoustic multilayer formalism (AMF). The following other models are available:
 - Roughness effects as turned into analytical equations by the Tel-Aviv group (section 5.2).
 - Analytical equations derived from a perturbation analysis (to 3rd or 5th order, section 5.5).
 - Elastic loading across point contacts (sections 2.7 and 5.3).
 - Coupled resonances (sections 2.8 and 5.4)

3.2 Fitting

Once a set of reasonable system parameters has been found, the quality of the model can be improved by a fit, that is, by a χ^2 -minimization. QTM offers a choice between the Simplex algorithm and the Levenberg-Marquardt algorithm for fitting.¹³ The Simplex algorithm is more robust, the Levenberg-Marquardt is more efficient when the numbers of fit parameters is large. Fitting is a bit of an art. It requires good starting values. It requires some experience, some understanding of the background, and a critical attitude in order to not over-interpret results.

χ^2 is a measure of the goodness of a fit. χ^2 is defined as

$$\chi^2 = \frac{1}{2n_{ovt} - n_{fitpar}} \sum_n w_n \left[\left(\frac{\Delta f_n - \Delta f_{n,fit}}{\delta f} \right)^2 + \left(\frac{\Delta \Gamma_n - \Delta \Gamma_{n,fit}}{\delta f} \right)^2 \right] \quad \text{Eq. 6}$$

n_{ovt} is the number of overtones included in the analysis. n_{fitpar} is the number of fit parameters. The factor of 2 before n_{ovt} occurs because every overtone contributes two data points (Δf and $\Delta \Gamma$). If only Δf or only $\Delta \Gamma$ are used for fitting (box above “Fit with” button), the factor of 2 is replaced by 1.

δf is the statistical uncertainty on Δf and $\Delta \Gamma$ on the fundamental. The uncertainty is about the same on f and Γ , hence only one parameter. QTM’s default value is $\delta f = 1$ Hz. This value can be changed by double-clicking onto the χ^2 symbol. A dialog will open. δf only affects the value of χ^2 , not the fit parameters, which make χ^2 minimal. If δf was estimated correctly and if χ^2 is of the order of unity, the quality of the fit is as good as it can get. χ^2 then is dominated by statistical noise. More often than not, systematic errors (rather than statistical noise) dominate χ^2 .

That leaves the question of how the weight w_n in Eq. 6 should depend on overtone order. If statistical noise dominates, the weights should be proportional to $1/n^2$ because the noise on Δf and $\Delta \Gamma$ is

roughly proportional to the overtone order n . However, the errors may be systematic rather than statistic. For that reason, QTM also allows for statistical weights proportional to n^{-1} and n^0 .

A few more comments:

- When a fit goes wrong, the fit parameters often go to values far outside the reasonable range. Recover the previous state with `<- Backup`.
- Parameters are turned into fit parameters by checking the squares next to them. QTM allows for a maximum of 6 fit parameters.
- Thickness, d , and density, ρ , cannot be active for fitting at the same time. d and ρ cannot be determined independently (see also section 4.1).
- The density of the bulk and the viscosity of the bulk cannot be fit parameters at the same time because the QCM only determines the viscosity-density product.
- The confidence range can be estimated with a procedure implemented the Form *chi² Landscape* (section 3.4).

3.3 Analyze entire files

Data from entire files are handled in the Form *Analyze Entire Files* (Figure 4). In a first step, import the data (either from the clipboard or from a file).

***** Make sure to have the option {Df[Hz], DG[Hz]} or {Df/n[Hz], DD[10⁻⁶]} set correctly. *****

Usually, one will skip some lines. QTM can handle a maximum of 10 000 lines, but it is advisable to work with smaller numbers for the sake of speed.

One may hide data points, data sets, or ranges of data.

One may select a new reference state.

Typically, one first picks one representative data set and finds a good set of system parameters using the Main Form. One then selects a range of data to be fitted. There is a choice with regard to the

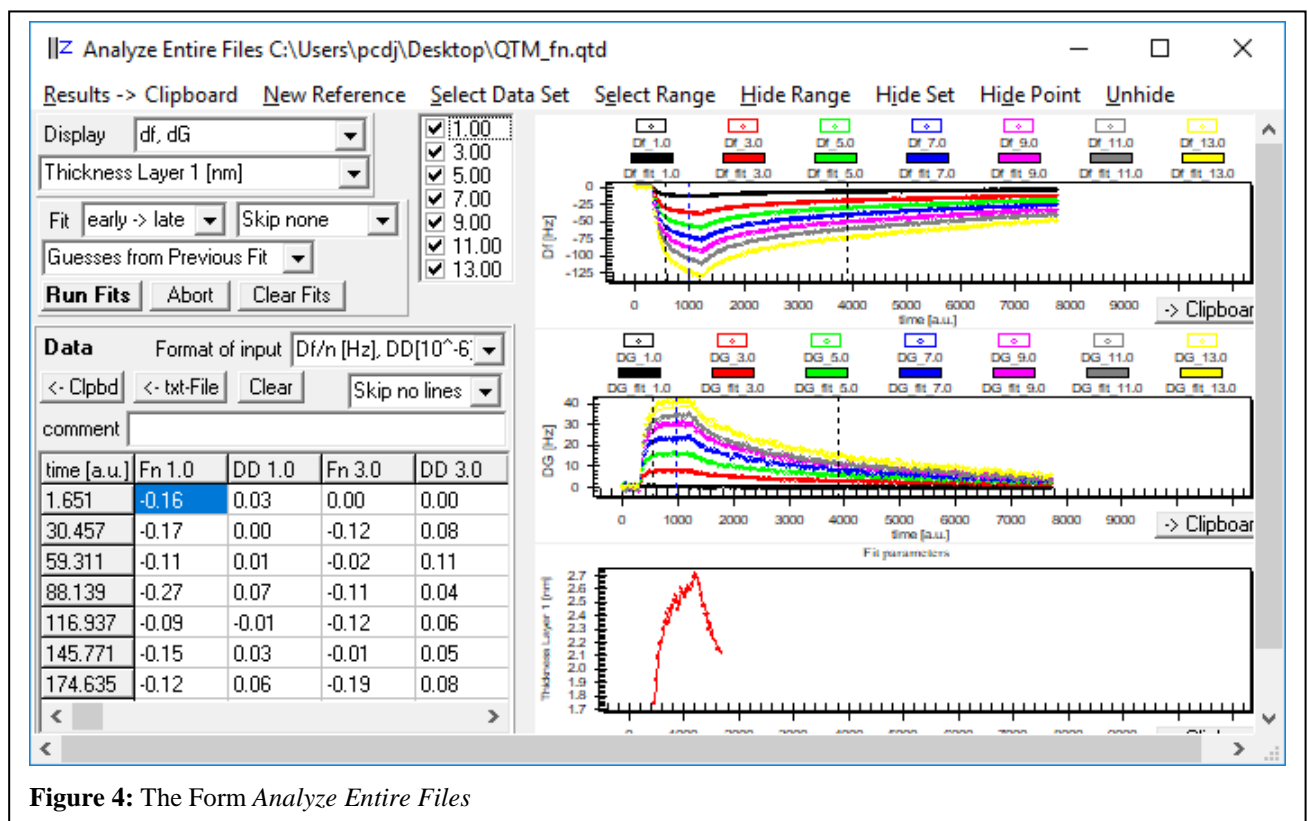


Figure 4: The Form *Analyze Entire Files*

guesses, from which the fit starts. The guess may be the result from the fit of the one data set, which was analyzed in detail. The guess may also be the result from the previous fit. The former method may go wrong when the properties of sample vary strongly over time and the one representative data set is not actually representative for the entire range of data. The latter method goes wrong when one fit fails. After one fit has failed, all following fits fail as well because of the poor values for the guess. If the latter option is chosen, it is sometimes helpful to proceed from late to early times because the sample slowly varies in its properties at the end of the experiment.

3.4 *Chi² landscape*

The confidence range is a bit of a thorny issue because systematic errors certainly exist. For a discussion of the matter in general see chapter 15.6 in Ref. 13. QTM implements a search for the confidence range in the Form *chi² Landscape* (Figure 5).

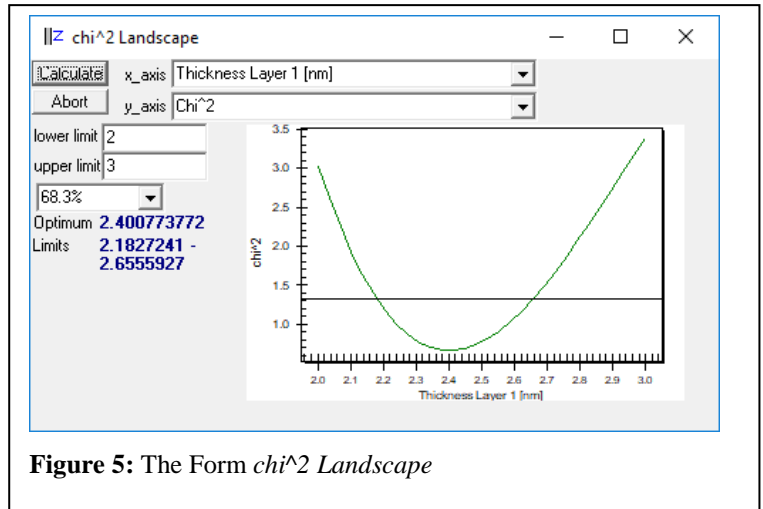


Figure 5: The Form *chi² Landscape*

QTM varies the parameter of interest in a certain range and does a fit, adjusting the *remaining* fit parameters, only. χ^2 resulting from this reduced fit is displayed versus the value of the respective parameter. This graph has a minimum at the value, where the first fit had converged. (After all, the fit undertaken from the Main Form had searched just that minimum.) Depending on how unique this result is, the χ^2 values increase more or less steeply to the left and right of the optimum. Select the confidence level in the respective box. QTM inserts horizontal lines into the graph and reports the confidence limits in blue.

QTM reports confidence limits based on the degree of confidence required. The factors in χ^2 corresponding to the different levels of confidence follow the table in section 15.6 in Ref. 13. For instance, if there is just one fit parameter, the values of χ^2 at the limits are

- $\chi^2_{limit} = 2 \chi^2_{min}$ for a confidence level of 68.3% (1σ)
- $\chi^2_{limit} = (1+2.71) \chi^2_{min}$ for a confidence level of 90%
- $\chi^2_{limit} = (1+6.63) \chi^2_{min}$ for a confidence level of 99%

The factors are larger in case there are more fit parameters.

QTM only reports limits, if χ^2 somewhere inside the search range increases to the values demanded by the chosen confidence level. If that is not the case, one may expand the search range – or accept that the uniqueness of the fit is poor.

3.5 *Further parameters entering the analysis*

There are parameters entering the analysis unrelated to the sample. These are:

- The frequency of the fundamental, f_0 . A typical value is $f_0 = 5$ MHz.

- The shear-wave impedance of AT-cut quartz. A typical value is $8.8 \cdot 10^6 \text{ kg m}^{-2} \text{ s}^{-1}$. There is some room for debate on the most suitable value of Z_q because of energy trapping.^f Other values of Z_q are needed for Langasite resonators¹⁴ and for torsional resonators.¹⁵
- The reference frequency for viscoelastic parameters ($\omega_{ref}/(2\pi)$) with ω_{ref} from Eq. 7. A typical value is $f_{ref} = 30 \text{ MHz}$. (Note: “ref” here is *not* the reference state.)

4 Some Details of the Machinery

4.1 Thickness versus mass per unit area

On a fundamental level, the QCM cannot independently determine the thickness and the density of a layer. Only the product of the two (the mass per unit area) enters the equations of the AMF. QTM nevertheless displays the thickness because the density often is known with good accuracy and because many users are more familiar with the unit nm than with the unit $\mu\text{g}/\text{cm}^2$. (If the density is $1 \text{ g}/\text{cm}^3$, $1 \mu\text{g}/\text{cm}^2$ correspond to a thickness of 10 nm.) Again, the derived thickness depends on the chosen density.

QTM uses the term "mass" for "mass per unit area". The unit is $\mu\text{g}/\text{cm}^2$. QTM displays the mass per unit area, after the user double-clicks onto the field showing the layer thickness.

4.2 Representation of viscoelasticity

Different parameters are in use to quantify viscoelasticity. QTM offers a choice between

- the shear modulus \tilde{G}
- the shear compliance \tilde{J}
- the viscosity $\tilde{\eta}$.

The three are related as $\tilde{J} = 1/\tilde{G}$ and $\tilde{G} = i\omega\tilde{\eta}$.^g \tilde{G} and $\tilde{\eta}$ are mostly used for solid and liquid media, respectively. QTM also offers the parameter \tilde{J} , because J' and J'' enter the frequency shift and the shift in bandwidth separately, if the film is much thinner than the wavelength of sound (see eqs. 10.1.10 and 10.2.6 in [3], see also Eq. 11 in this text). Arguably, the QCM senses softness rather than stiffness because soft samples behave peculiarly, while stiff samples look like Sauerbrey layers. In all three cases (\tilde{G} , \tilde{J} , or $\tilde{\eta}$), there is a choice to express the complex parameters as $\tilde{G} = G' + iG''$ or as $\tilde{G} = |G| \exp(i\delta_L)$ (analogous relations for \tilde{J} and $\tilde{\eta}$). QTM actually uses $\tan \delta_L$ for fitting rather than δ_L . $\tan \delta_L$ is the same as the loss tangent, if $\tilde{G} =$ or \tilde{J} are employed. (δ_L is the inverse loss tangent for $\tilde{\eta}$.)

The user can choose between the different representations in the boxes on the right-hand side. When the user changes the representation, QTM attempts to change the values accordingly. This is less-than-perfect, because a power law in one representation does not always translate to a power law in another representation.

Importantly, the viscoelastic parameters depend on frequency. This may create the impression that the problem was underdetermined because there are separate values of G' and G'' for every single overtone. However, the frequency dependence of G' and G'' usually is smooth. QTM assumes power laws of the form

^f Choose $f_0 = 4.95 \text{ MHz}$ and $Z_q = 8.769382 \cdot 10^6 \text{ kg m}^{-2} \text{ s}^{-1}$ if you want to achieve exact agreement with QTools.

^g G' is *not* equal to $1/J'$. The relation is $G' = J'/(J'^2 + J''^2)$. Similar relations hold for the other conversions.

$$G'(f) = G'_{ref} \left(\frac{f}{f_{ref}} \right)^{\beta'} \quad G''(\omega) = G''_{ref} \left(\frac{f}{f_{ref}} \right)^{\beta''}$$

Analogous relations hold for \tilde{J} and $\tilde{\eta}$.

Note: These power laws also hold, if the complex variables are expressed in polar form. They *always* apply to the real part and the imaginary part, never to the absolute value and $\tan \delta$.

A note on terminology: Eq. 7 and QTM use the frequency, f , related to the angular frequency by $\omega = 2\pi f$. This text also often uses the angular frequency ω . Occasionally, the reader needs to remember the factor of 2π .

There is a problem with power laws: A power law behavior in $G'(\omega)$ and $G''(\omega)$ does not translate to a power law after converting to $J'(\omega)$ and $J''(\omega)$. In consequence, the frequency shifts, which QTM computes, slightly differ, when switching between representations.

The Kramers-Kronig relations pose limits on β' and β'' :

- If the modulus is used (G' and G''), one has $0 < \beta' < 2$ and $-1 < \beta'' < 1$.
- If the compliance is used (J' and J''), one has $-2 < \beta' < 0$ and $-1 < \beta'' < 1$.
- If the viscosity is used (η' and η''), one has $-2 < \beta' < 0$ and $-1 < \beta'' < 1$.

These limits are implemented as default limits in the Limits Form.

4.3 Reference state

Any frequency shift in QTM is to be understood as a frequency shift relative to the frequency in the respective reference state. Make sure that QTM uses the correct reference state. The parameters of the reference state can be edited in the Reference Form. One may also turn some state into the reference state by clicking the button \rightarrow *Reference*.

For the coupled resonance and for effects of elastic stiffness, QTM only offers the trivial reference state.

The reference state cannot be rough.

QTM forces the user to choose the same viscoelastic parameters (such as $\{J', J''\}$ or $\{G', G''\}$) in the reference state and the state with the sample. There is a reason to do this. A power law in $\{J', J''\}$ and a power law in $\{G', G''\}$ are not completely equivalent (unless the exponents are zero). If the reference state and the state with the sample use different sets of viscoelastic parameters, there is the danger that a nonzero frequency shift is predicted simply because the choices of variables are unequal. This must be avoided.

4.4 Discard data from the fundamental

For a number of (poorly understood) reasons, the frequency shift measured on the fundamental often does not match the expectations well and the data from the fundamental might just as well be discarded. Depending on the details, data from the 3rd overtone can be problematic as well.

4.5 Film resonances

Films with a thickness of about a quarter of the wavelength of sound produce a film resonance (section 10.1 in [3]). An example is the tangent in Eq. 13. If the film shows sufficient damping, Eq. 13 can be trusted. Otherwise, the load becomes large and the SLA does no longer hold at the film resonance. Around the film resonance, there are two modes, rather than one. One can see this as a

sudden jump of the frequency shift in a swelling experiment. As swelling proceeds, the lower mode becomes weaker and weaker. At some point, the instrument can no longer find the lower mode and searches for other modes in the vicinity. Eventually it finds the higher mode (higher in frequency). The frequency shift then jumps upwards.

Even in cases, where the film resonance is so broad that there is no mode splitting, the agreement between the AMF and the experimental data has often poor in the past. Presumably this happens, because mode splitting still affects the data in one way or another.

4.6 Electrode effects

For the determination of the viscoelastic properties of films in the dry state, it is essential to properly include the thickness and the modulus of the front electrode into the reference state. These have to be known with good accuracy. Typically, layer 1 then is the electrode, layer 2 is the sample. Why electrodes are of such importance in the dry state, is explained in Ref. 16.

4.7 Viscoelastic profiles

In principle, viscoelastic profiles (for instance produced by a polymer brush) may be covered by the acoustic multilayer formalism, using many layers. There was such an option in the previous version, but it was removed because uniqueness of the fit proved to be problematic. Actually, there is a rather easy way to predict Δf and $\Delta \Gamma$ for such situation, solving the underlying partial differential equation. Sample code is contained in “SolveWaveEquationViscoElasticProfiles.nb”. Mathematica solves the wave equation for continuous profiles of $G'(z)$, $G''(z)$, and $\rho(z)$ and derives the shifts of frequency and bandwidth from the solution. The core of the program is a few lines long. For more details see sections 10.6 and 10.8 in [3].

5 Underlying Equations

5.1 Layer systems

QTM computes the acoustic load induced by layer systems following the matrix formalism as described in section 5 in [3]. For simple layer systems (1 or 2 layers), there are explicit equations, provided below. For a single layer in air, one has

$$\frac{\Delta \tilde{f}}{f_0} = \frac{-1}{\pi Z_q} \tilde{Z}_f \tan(k_f d_f) \quad \text{Eq. 8}$$

Taylor expansion of Eq. 8 to 1st order in film thickness, d_f , yields the Sauerbrey result (section 10.1 in [3]). There is a twist with regard to the Taylor expansion to 3rd order in d_f . This expansion reveals finite-compliance effects in the thin-film limit. Taylor expansion of Eq. 8 to 3rd order in film thickness yields

$$\frac{\Delta \tilde{f}}{f_0} = \frac{-\omega m_f}{\pi Z_q} \left(1 + \frac{(n\pi)^3}{3} \frac{Z_q^2}{\tilde{Z}_f^2} \frac{m_f^2}{m_q^2} \right) \quad \text{Eq. 9}$$

The perturbation calculation shows that the correct equation is

$$\frac{\Delta \tilde{f}}{f_0} = \frac{-\omega m_f}{\pi Z_q} \left(1 + \frac{(n\pi)^3}{3} \left(\frac{Z_q^2}{\tilde{Z}_f^2} - 1 \right) \frac{m_f^2}{m_q^2} \right) \quad \text{Eq. 10}$$

Expressed as a function of the film's viscoelastic compliance, this result reads as

$$\frac{\Delta \tilde{f}}{f_0} = \frac{-\omega m_f}{\pi Z_q} \left(1 + \frac{(n\pi)^3}{3} \left(\frac{\tilde{J}_f}{\rho_f} Z_q^2 - 1 \right) \frac{m_f^2}{m_q^2} \right) \quad \text{Eq. 11}$$

If the film's stiffness is comparable to the stiffness of the crystal (if $Z_f \approx Z_q$), the difference is substantial. If $\Delta f(n)$ is naively analyzed with Eq. 9, one may easily find negative values for G' .

For a single layer in a liquid one has

$$\frac{\Delta \tilde{f}}{f_0} = \frac{-\tilde{Z}_f \tilde{Z}_f \tan(\tilde{k}_f d_f) - i \tilde{Z}_{liq}}{\pi Z_q \tilde{Z}_f + i \tilde{Z}_{liq} \tan(\tilde{k}_f d_f)} \quad \text{Eq. 12}$$

Taylor expansion of 1st order in the mass per unit area yields

$$\Delta \tilde{f} = -\frac{2f_0 f}{Z_q} m_f \left(1 - \frac{Z_{liq}^2}{Z_f^2} \right) = -\frac{2f_0 f}{Z_q} m_f \left(1 - \frac{J_f}{\rho_f} Z_{liq}^2 \right) \quad \text{Eq. 13}$$

Even for very thin films, this equation is different from the Sauerbrey equation. The term in brackets is sometimes associated with the “missing mass effect”.¹⁷ The author calls it the “finite compliance effect”.¹⁶ Finite compliance lowers the apparent mass, if analyzed with the Sauerbrey equation.

The current version of QTM allows for a maximum of two layers. The AMF result for a system of two layers embedded in a liquid still fits into one line:

$$\frac{\Delta \tilde{f}}{f_F} = \frac{-Z_e Z_f (Z_e \tan(k_e d_e) + Z_f \tan(k_f d_f)) + i Z_{liq} (Z_e \tan(k_f d_f) \tan(k_e d_e) - Z_f)}{\pi Z_q Z_f (Z_e - Z_f \tan(k_f d_f) \tan(k_e d_e)) + i Z_{liq} (Z_e \tan(k_f d_f) + Z_f \tan(k_e d_e))} \quad \text{Eq. 14}$$

Eq. 8, Eq. 12, and Eq. 14 can be programmed as fit functions into Excel. The Excel solver should produce the same fits as QTM.

5.2 Roughness

Shallow roughness on small scales ($h_r \ll l_r$, $h_r \ll \delta$, $l_r \ll \delta$) is represented as

$$\begin{aligned} \frac{\Delta f}{f_0} &= \frac{-Z''_{liq,eff}}{\pi Z_q} \approx \frac{-1}{\pi Z_q} \sqrt{\frac{\rho_{liq} \omega \eta_{liq}}{2}} \left(1 + 3\sqrt{\pi} \frac{h_r^2}{l_r \delta} - 2 \frac{h_r^2}{\delta^2} \right) \\ \frac{\Delta \Gamma}{f_0} &= \frac{Z'_{liq,eff}}{\pi Z_q} \approx \frac{1}{\pi Z_q} \sqrt{\frac{\rho_{liq} \omega \eta_{liq}}{2}} \left(1 + 2 \frac{h_r^2}{\delta^2} \right) \end{aligned} \quad \text{Eq. 15}$$

Shallow roughness on large scales ($h_r \ll l_r$, $h_r \ll \delta$, $l_r \gg \delta$) is represented as

$$\begin{aligned} \frac{\Delta f}{f_0} &= \frac{-Z''_{liq,eff}}{\pi Z_q} \approx \frac{-1}{\pi Z_q} \sqrt{\frac{\rho_{liq} \omega \eta_{liq}}{2}} \left(1 + 2 \frac{h_r^2}{l_r^2} + \sqrt{\pi} \frac{h_r^2}{l_r \delta} \right) \\ \frac{\Delta \Gamma}{f_0} &= \frac{Z'_{liq,eff}}{\pi Z_q} = \frac{1}{\pi Z_q} \sqrt{\frac{\rho_{liq} \omega \eta_{liq}}{2}} \left(1 + 2 \frac{h_r^2}{l_r^2} \right) \end{aligned} \quad \text{Eq. 16}$$

Non-shallow roughness modeled with Darcy flow follows the equation

$$Z_{liq,eff} \approx \sqrt{\frac{\rho_{liq} \omega \eta}{2}} \left[\frac{1}{q_0} + \frac{L}{\xi_H^2 q_1^2} - \frac{1}{W} \frac{L}{\xi_H^2 q_1^2} \left(\frac{2q_0}{q_1} [\cosh(q_1 L) - 1] + \sinh(q_1 L) \right) \right] \quad \text{Eq. 17}$$

$$q_0 = \sqrt{\frac{i\omega\rho}{\eta}}, \quad q_1 = \sqrt{q_0^2 + \xi_H^{-2}}, \quad W = q_1 \cosh(q_1 L) + q_0 \sinh(q_1 L)$$

QTM assigns the effective impedance to the bulk medium. In this way, roughness can be part of the acoustic multilayer formalism (Figure 2).

5.3 Elastic loading across point contacts

In the most simple version of elastic coupling, one has the relation (section 11 in [3])

$$\frac{\Delta \tilde{f}}{f_0} = \frac{1}{\pi Z_q} \frac{n_p}{A} \frac{\tilde{\kappa}}{\omega} \quad \text{Eq. 18}$$

$\tilde{\kappa}$ is a complex contact stiffness, n_p/A is the number of contacts per unit area. The combination of parameters $(n_p/A)\tilde{\kappa}$ can be collected into an “effective contact stiffness” $\tilde{\kappa}_{eff}$. The real and the imaginary part are expressed as

$$\tilde{\kappa} = \kappa' + i\omega\xi = \kappa'(1 + i \tan \delta_L) \quad \text{Eq. 19}$$

ξ is the drag coefficient of a dashpot mounted in parallel to the spring. The contact here is modeled as a Voigt-element in the sense of rheology. $\tan \delta_L$ is the loss tangent (compare to section 4.2). The loss tangent is the fit parameter.

QTM goes beyond this simple model in two regards. Firstly, it allows for an offset in $\Delta f/n$ and $\Delta \Gamma/n$:

$$\frac{\Delta \tilde{f}}{f_0} = \frac{1}{\pi Z_q} \frac{\tilde{\kappa}_{eff}}{\omega} + n \left(\frac{\Delta \tilde{f}}{n} \right)_{off} \quad \text{Eq. 20}$$

Also, it allows for viscoelastic dispersion on the elastic stiffness, κ'_{eff} , and on the drag coefficient, ξ_{eff} following

$$\kappa'_{eff}(f) = \kappa'_{ref}(f_{ref}) \left(\frac{f}{f_{ref}} \right)^{\beta'} \quad \xi_{eff}(f) = \xi_{ref}(f_{ref}) \left(\frac{f}{f_{ref}} \right)^{\beta'} \quad \text{Eq. 21}$$

The situation is similar to what is done in the case of viscoelastic dispersion. The power law exponents are called “PL exp” in QTM.

5.4 Coupled resonances

For a discussion of coupled resonances, see chapter 11.5 in [3]. The frequency shift induced by an adhering particle with its own “particle resonance frequency” is given as

$$\frac{\Delta \tilde{f}}{f_0} = \frac{-1}{\pi Z_q} f_{OS} \omega M_p \frac{\tilde{\omega}_p^2}{\tilde{\omega}_{p,0}^2 - \omega^2} \quad \text{Eq. 22}$$

$\tilde{\omega}_{p,0}$ is the particle resonance frequency. Plotting Δf and $\Delta\Gamma$ versus n , one again finds a resonance curve.

Eq. 22 assumes the spring and the dashpot to operate in parallel (assumes a ‘‘Voigt-type’’ link). For the Maxwell-type link see below.

$\tilde{\omega}_{p,0}$ is defined by the relation

$$\tilde{\omega}_{p,0}^2 = \frac{\kappa_p}{M_p} + \frac{i\omega\xi_p}{M_p} \quad \text{Eq. 23}$$

κ_p is the elastic stiffness of the contact and ξ_p is the drag coefficient of the corresponding dashpot. One defines a damping constant, γ_p , as

$$\gamma_p = \frac{\xi_p}{M_p} \quad \text{Eq. 24}$$

The parameters used by QTM are

$$f_{p,0}' = \frac{1}{2\pi} \sqrt{\omega_{p,0}'^2} = \frac{1}{2\pi} \sqrt{\frac{\kappa_p}{M_p}} \quad \text{Eq. 25}$$

$$f_{p,0}'' = \frac{1}{2\pi} \sqrt{\omega_{p,0}''^2} = \frac{1}{2\pi} \gamma_p$$

The right-hand side contains the roots of real and the imaginary parts of $\tilde{\omega}_{p,0}^2$, not the other way round. Taking the root first leads to the ‘‘ringing frequency’’. $f_{p,0}'$ is the undamped resonance frequency, which differs from the ringing frequency (eq. 4.1.18 in [3]). While the difference is marginal for the resonance frequency of the QCM, it can be substantial for the particle resonance frequency,

If the spring and the dashpot are arranged in series (‘‘Maxwell-type’’ link), one has¹¹

$$\tilde{\omega}_{p,0,Maxwell}^2 = \frac{1}{M_p} \left(\frac{1}{\kappa_p} + \frac{1}{i\omega\xi_p} \right)^{-1} \quad \text{Eq. 26}$$

Eq. 22 is then replaced by

$$\frac{\Delta\tilde{f}}{f_0} = \frac{-1}{\pi Z_q} f_{os} \omega M_p \frac{1}{1 - \frac{\omega^2}{\omega_p^2} + \frac{i\omega}{\gamma_p}} \quad \text{Eq. 27}$$

There are a few complications:

- In most experiments, the parameters entering Eq. 22 (or Eq. 27) will not be the same for all particles. There may be distributions in $f_{p,0}'$, $f_{p,0}''$, and M_p . QTM seeks a compromise between realistic modeling, on the one hand, and simplicity, on the other. It allows for a Gaussian distribution in $f_{p,0}'$. The parameters $f_{p,0}''$ and M_p assume a single value. Given the distribution, there are two fit parameters associated with $f_{p,0}'$ which are the center of the distribution and its width. Because the Gaussian distribution is cut off at $f_{p,0}' = 0$, the center of the Gaussian is not the average of $f_{p,0}'$. The average is calculated separately (called $\langle f_p \rangle$ [MHz] in QTM).

- For spheres adsorbed from the liquid phase, there will be sources of frequency shifts other than the coupled resonance. In order to account for these, QTM allows for an offset in $\Delta f/n$ and an offset in $\Delta\Gamma/n$.
- There is a prefactor in Eq. 22, which is the “oscillator strength”, f_{os} (see section 11.5 in [3]). Also, the number of particles per unit area may be unknown. QTM absorbs the combination of parameters $f_{os}N_P M_P$ into one fit parameter, which is the effective mass, m_{eff} .

We now have the parameters of the model assembled. There are 8 parameters, which are

- | | |
|---|---|
| - The apparent mass per unit area | m_{eff} [$\mu\text{g}/\text{cm}^2$] |
| - The center of the Gaussian distribution in $f_{p,0}'$ | f_{CR} [MHz] |
| - The width of the distribution in $f_{p,0}'$ | Het. Linew. [MHz] |
| - The damping coefficient, $\gamma_p/2\pi$ | Hom. Linew. [MHz] |
| - The offset in $\Delta f/n$ | Df/n Off [Hz] |
| - The offset in $\Delta\Gamma/n$ | DG/n Off [Hz] |
| - A power law exponent for κ_{eff}' | PL exp k' |
| - A power law exponent for ξ_{eff} | PL exp xi |

For the Voigt-type link, QTM fits the data with the equation

$$\Delta\tilde{f} \approx -m_{eff} \frac{f_0}{\pi Z_q} \omega \int_0^{\infty} g(f_{p,0}') \frac{f_{p,0}'^2 + i\omega f_{p,0}' - \omega^2}{(f_{p,0}'^2 + i\omega f_{p,0}' - \omega^2)^2} df_{p,0}' \quad \text{Eq. 28}$$

Replace the ratio by the corresponding ratio from Eq. 27 for the Maxwell-type link.

The distribution function $g(f_{p,0}')$ is

$$g(f_{p,0}') = \frac{1}{Z_{norm}} \exp\left(-\frac{(f_{p,0}' - f_{p,0,cen}')^2}{2\sigma^2}\right) \quad \text{Eq. 29}$$

Z_{norm} takes care of normalization. It is computed numerically.

QTM allows to also use a single real part of the particle resonance frequency (“Single omP“ rather than „PolyDis in omP“ in the respective box). Internally, QTM simply uses a very narrow distribution in this case.

5.5 Perturbation analysis

The equations implemented by QTM are given below. We start with abbreviated notation:

Index e : first layer (“electrode”)

Index f : second layer (“film”)

Index liq : bulk medium (“liquid”)

Reduced masses: $\mu_e = m_e/m_q$, $\mu_f = m_f/m_q$

Reduced shear-wave impedances

$$\zeta_e(\omega) = \frac{Z_q^2}{Z_e^2(\omega)} - 1, \quad \zeta_f(\omega) = \frac{Z_q^2}{Z_f^2(\omega)} - 1, \quad \xi_{liq}(\omega) = \frac{Z_{liq}(\omega)}{Z_q} \quad \text{Eq. 30}$$

5.5.1 Semi-infinite liquid (can be a viscoelastic medium)

$$\text{SLA: } \frac{\Delta \tilde{f}}{f_0} = \frac{i}{\pi Z_q} \tilde{Z}_{liq} \quad \text{Eq. 31}$$

$$\text{3rd order: } \frac{\Delta \tilde{f}}{f_{ref}} = \frac{i}{n\pi} \left(\xi_{liq} + \frac{1}{3} \xi_{liq}^3 \right)$$

$$\text{5th order: } \frac{\Delta \tilde{f}}{f_{ref}} = \frac{i}{n\pi} \left(\xi_{liq} + \frac{1}{3} \xi_{liq}^3 + \frac{1}{5} \xi_{liq}^5 \right)$$

5.5.2 Viscoelastic film in air

$$\text{SLA: } \frac{\Delta \tilde{f}}{f_0} = \frac{-Z_f}{\pi Z_q} \tan(k_f d_f) \quad \text{Eq. 32}$$

$$\text{3rd order: } \frac{\Delta \tilde{f}}{f_{ref}} = -\mu_f + \mu_f^2 - \left(1 + \frac{1}{3} (n\pi)^2 \zeta_f \right) \mu_f^3$$

5th order:

$$\begin{aligned} \frac{\Delta \tilde{f}}{f_{ref}} = & -\mu_f + \mu_f^2 - \left(1 + \frac{(n\pi)^2}{3} \zeta_f \right) \mu_f^3 + \left(1 + \frac{4(n\pi)^2}{3} \zeta_f \right) \mu_f^4 \\ & - \left(1 + \frac{10(n\pi)^2}{3} \zeta_f + \frac{(n\pi)^4}{15} (1 - 2\zeta_f) \zeta_f \right) \mu_f^5 \end{aligned}$$

5.5.3 Viscoelastic film in liquid

$$\text{SLA: } \frac{\Delta \tilde{f}}{f_0} = \frac{-1}{\pi Z_q} \frac{Z_f \tan(k_f d_f) - i Z_{liq}}{Z_f + i Z_{liq} \tan(k_f d_f)}$$

Eq. 33

3rd Order:

$$\begin{aligned} \frac{\Delta \tilde{f}}{f_{ref}} &= \frac{i}{n\pi} \left(\xi_{liq} + \frac{1}{3} \xi_{liq}^3 \right) - \left(1 + \frac{i \xi_{liq}}{n\pi} - \zeta_e \xi_{liq}^2 \right) \mu_f \\ &+ \left(1 + \left(\frac{i}{n\pi} + i n \pi \zeta_f \right) \xi_{liq} \right) \mu_f^2 - \left(1 + \frac{(n\pi)^2}{3} \zeta_f \right) \mu_f^3 \end{aligned}$$

5th Order

$$\begin{aligned} \frac{\Delta \tilde{f}}{f_{ref}} &= \frac{i \xi_{liq}}{n\pi} + \frac{i \xi_{liq}^3}{3n\pi} + \frac{i \xi_{liq}^5}{5n\pi} + \left(-1 - \frac{i \xi_{liq}}{n\pi} + \zeta_f \xi_{liq}^2 + \frac{(-5i + 15i \zeta_f) \xi_{liq}^3}{15n\pi} + \zeta_f \xi_{liq}^4 \right) \mu_f + \\ &\left(1 + \left(\frac{i}{n\pi} + i n \pi \zeta_f \right) \xi_{liq} - 4 \zeta_f \xi_{liq}^2 + \frac{(5i - 45i \zeta_f)}{15n\pi} + \frac{(15i \pi^2 \zeta_f - 15i \pi^2 \zeta_f^2)}{15n\pi} \xi_{liq}^3 \right) \mu_f^2 + \\ &\left(-1 - \frac{1}{3} n^2 \pi^2 \zeta_f + \left(-\frac{i}{n\pi} - 4i n \pi \zeta_f \right) \xi_{liq} + \left(10 \zeta_f + \frac{n^2 (-10 \pi^3 \zeta_f + 20 \zeta_f^2)}{15\pi} \right) \xi_{liq}^2 \right) \mu_f^3 + \\ &\left(1 - \frac{4}{3} n^2 \pi^2 \zeta_f + \left(\frac{i}{n\pi} + 10i n \pi \zeta_f + \frac{n^3 (-5 \pi^4 \zeta_f + 10 \pi^4 \zeta_f^2)}{15\pi} \right) \xi_{liq} \right) \mu_f^3 + \\ &\left(-1 - \frac{10}{3} n^2 \pi^2 \zeta_f - \frac{1}{15} n^4 \pi^4 \zeta_f (-1 + 2 \zeta_f) \right) \mu_f^5 \end{aligned}$$

5.5.4 Two viscoelastic films in air

SLA-Result:

$$\frac{\Delta \tilde{f}}{f_F} = \frac{-1}{\pi Z_q} \frac{Z_f \tan(k_f d_f) + Z_e \tan(k_e d_e)}{1 - Z_f / Z_e \tan(k_f d_f) \tan(k_e d_e)}$$

Eq. 34

Perturbation analysis, 3rd order:

$$\begin{aligned} \frac{\Delta f^*}{f_0} &= -\mu_e + \mu_e^2 - \left(1 + \frac{(n\pi)^2}{3} \zeta_e \right) \mu_e^3 - \left(1 - 2\mu_e + 3 \left(1 + \frac{(n\pi)^2}{3} \zeta_e \right) \mu_e^2 \right) \mu_f \\ &+ \left(1 - 3 \left(1 + \frac{(n\pi)^2}{3} \zeta_e \right) \mu_e \right) \mu_f^2 - \left(1 + \frac{(n\pi)^2}{3} \zeta_f \right) \mu_f^3 \end{aligned}$$

Eq. 35

Perturbation analysis, 5th order:

$$\begin{aligned}
\frac{\Delta \tilde{f}}{f_{ref}} = & -\mu_e + \mu_e^2 + \left(-1 - \frac{1}{3}n^2\pi^2\zeta_e\right)\mu_e^3 + \left(1 + \frac{4}{3}n^2\pi^2\zeta_e\right)\mu_e^4 + \\
& \left(-1 - \frac{10}{3}n^2\pi^2\zeta_e - \frac{1}{15}n^4\pi^4\zeta_e(-1+2\zeta_e)\right)\mu_e^5 + \\
& \left(-1+2\zeta_e + (-3-n^2\pi^2\zeta_e)\mu_e^2 + \left(4 + \frac{16}{3}n^2\pi^2\zeta_e\right)\mu_e^3 + \left(-5 - \frac{50}{3}n^2\pi^2\zeta_e - \frac{1}{3}n^4\pi^4\zeta_e(-1+2\zeta_e)\right)\mu_e^4\right)\mu_f + \\
& \left(1 + (-3-n^2\pi^2\zeta_e)\mu_e + (6+8n^2\pi^2\zeta_e)\mu_e^2 + \left(-10 - \frac{100}{3}n^2\pi^2\zeta_e - \frac{2}{3}n^4\pi^4\zeta_e(-1+2\zeta_e)\right)\mu_e^3\right)\mu_f^2 + \\
& \left(-1 - \frac{1}{3}n^2\pi^2\zeta_f + \left(4 + \frac{4}{3}n^2\pi^2(3\zeta_e + \zeta_f)\right)\mu_e + \left(-10 - \frac{1}{3}n^4\pi^4\zeta_e(-2+3\zeta_e + \zeta_f)\right) - \frac{10}{3}n^2\pi^2(9\zeta_e + \zeta_f)\mu_e^2\right)\mu_f^3 + \\
& \left(1 + \frac{4}{3}n^2\pi^2\zeta_f + \left(-5 - \frac{1}{3}n^4\pi^4\zeta_e(-1+2\zeta_f) - \frac{10}{3}n^2\pi^2(3\zeta_e + 2\zeta_f)\right)\mu_e\right)\mu_f^4 + \\
& \left(-1 - \frac{10}{3}n^2\pi^2\zeta_f - \frac{1}{15}n^4\pi^4\zeta_f(-1+2\zeta_f)\right)\mu_f^5
\end{aligned}$$

Eq. 36

5.5.5 Two viscoelastic films in a liquid

SLA-Result:

$$\frac{\Delta \tilde{f}}{f_F} = \frac{-Z_e Z_f (Z_e \tan(k_e d_e) + Z_f \tan(k_f d_f)) + iZ_{liq} (Z_e \tan(k_f d_f) \tan(k_e d_e) - Z_f)}{\pi Z_q Z_f (Z_e - Z_f \tan(k_f d_f) \tan(k_e d_e)) + iZ_{liq} (Z_e \tan(k_f d_f) + Z_f \tan(k_e d_e))}$$

Eq. 37

Perturbation analysis, 3rd order:

$$\begin{aligned}
\frac{\Delta \tilde{f}}{f_{ref}} = & \frac{i}{n\pi} \left(\xi_{liq} + \frac{1}{3} \xi_{liq}^3 \right) - \left(1 + \frac{i}{n\pi} \xi_{liq} - \zeta_e \xi_{liq}^2 \right) \mu_e + \left(1 + \left(\frac{i}{n\pi} + i n \pi \zeta_e \right) \xi_{liq} \right) \mu_e^2 \\
& - \left(1 + \frac{1}{3} (n\pi)^2 \zeta_e \right) \mu_e^3 \\
& - \left(1 + \frac{i}{n\pi} \xi_{liq} - \zeta_f \xi_{liq}^2 - 2 \left(1 + \left(\frac{i}{n\pi} + i n \pi \zeta_e \right) \xi_{liq} \right) \mu_e + 3 \left(1 + \frac{1}{3} (n\pi)^2 \zeta_e \right) \mu_e^2 \right) \mu_f \\
& + \left(1 + \left(\frac{i}{n\pi} + i n \pi \zeta_f \right) \xi_e - 3 \left(1 + \frac{1}{3} (n\pi)^2 \zeta_e \right) \mu_e \right) \mu_f^2 \\
& - \left(1 + \frac{1}{3} (n\pi)^2 \zeta_f \right) \mu_f^3
\end{aligned}$$

Eq. 38

Perturbation analysis, 5th order:

$$\begin{aligned}
\frac{\Delta \tilde{f}}{f_{ref}} = & \frac{i \xi_{liq}}{n\pi} + \frac{i \xi_{liq}^3}{3n\pi} + \frac{i \xi_{liq}^5}{5n\pi} + \left(-1 - \frac{i \xi_{liq}}{n\pi} + \zeta_e \xi_{liq}^2 + \frac{(-5i+15i\zeta_e) \xi_{liq}^3}{15n\pi} + \zeta_e \xi_{liq}^4 \right) \mu_f + \\
& \left(1 + \left(\frac{i}{n\pi} + i n \pi \zeta_e \right) \xi_{liq} - 4 \zeta_e \xi_{liq}^2 + \left(\frac{5i-45i\zeta_e}{15n\pi} + \frac{n(15i\pi^2\zeta_e - 15i\pi^2\zeta_e^2)}{15n\pi} \right) \xi_{liq}^3 \right) \mu_e^2 + \\
& \left(-1 - \frac{1}{3} n^2 \pi^2 \zeta_e + \left(-\frac{i}{n\pi} - 4i n \pi \zeta_e \right) \xi_{liq} + \left(10\zeta_e + \frac{n^2(-10\pi^3\zeta_e + 20\pi^3\zeta_e^2)}{15\pi} \right) \xi_{liq}^2 \right) \mu_e^3 + \\
& \left(1 - \frac{4}{3} n^2 \pi^2 \zeta_e + \left(\frac{i}{n\pi} + 10i n \pi \zeta_e + \frac{1}{3} i n^3 \pi^3 \zeta_e (-1+2\zeta_e) \right) \xi_{liq} \right) \mu_e^4 + \\
& \left(-1 - \frac{10}{3} n^2 \pi^2 \zeta_e - \frac{1}{15} n^4 \pi^4 \zeta_e (-1+2\zeta_e) \right) \mu_f^5 + \\
& \left(-1 - \frac{i \xi_{liq}}{n\pi} + \zeta_f \xi_{liq}^2 + \frac{(-5i+15i\zeta_f) \xi_{liq}^3}{15n\pi} + \zeta_f \xi_{liq}^4 + \right. \\
& \quad \left. \left(2 + \left(\frac{2i}{n\pi} + 2i n \pi \zeta_e \right) \xi_{liq} + \frac{(-90\pi\zeta_e - 30\pi\zeta_f) \xi_{liq}^2}{15\pi} + \left(\frac{10i-60i\zeta_e - 30i\zeta_f}{15n\pi} - 2i n \pi \zeta_e (-1+\zeta_f) \right) \xi_{liq}^3 \right) \mu_e + \right. \\
& \quad \left. \left(-3n^2 \pi^2 \zeta_e + \left(-\frac{3i}{n\pi} - 12i n \pi \zeta_e \right) \xi_{liq} + \left(\frac{n^2(45\pi^3\zeta_e^2 + 15\pi^2\zeta_e(-2+\zeta_f))}{15\pi} + \frac{405\pi\zeta_e + 45\zeta_f}{15\pi} \right) \xi_{liq}^2 \right) \mu_e^2 + \right. \\
& \quad \left. \left(4 + \frac{16}{3} n^2 \pi^2 \zeta_e + \left(\frac{4i}{n\pi} + 40i n \pi \zeta_e + \frac{4}{3} i n^3 \pi^3 \zeta_e (-1+2\zeta_e) \right) \xi_{liq} \right) \mu_e^3 + \left(-5 - \frac{50}{3} n^2 \pi^2 \zeta_e - \frac{1}{3} n^4 \pi^4 \zeta_e (-1+2\zeta_e) \right) \mu_e^4 \right) \mu_f + \\
& \left(1 + \left(-\frac{i}{n\pi} + i n \pi \zeta_f \right) \xi_{liq} - 4 \zeta_f \xi_{liq}^2 + \left(\frac{5i-45i\zeta_f}{15n\pi} + \frac{n(15i\pi^2\zeta_f - 15i\pi^2\zeta_f^2)}{15\pi} \right) \xi_{liq}^3 + \right. \\
& \quad \left. \left(-3 - n^2 \pi^2 \zeta_e + \left(-\frac{3i}{n\pi} - 3i n \pi \zeta_e (3\zeta_e + \zeta_f) \right) \xi_{liq} + 2n^2 \pi^2 \zeta_e (-1+2\zeta_f) + \frac{270\pi\zeta_e + 180\zeta_f}{15\pi} \right) \xi_{liq}^2 \right) \mu_e + \\
& \quad \left(6 + 8n^2 \pi^2 \zeta_e + \left(\frac{6i}{n\pi} + i n^3 \pi^3 \zeta_e (-2+3\zeta_e + \zeta_f) + \frac{n(810i\pi^2\zeta_e + 90i\pi^2\zeta_f^2)}{15\pi} \right) \xi_{liq} \right) \mu_e^2 + \\
& \quad \left(-10 + \frac{100}{3} n^2 \pi^2 \zeta_e + \frac{2}{3} n^4 \pi^4 \zeta_e (-1+2\zeta_e) \right) \mu_e^3 \right) \mu_f^2 + \\
& \left(-1 - \frac{1}{3} n^2 \pi^2 \zeta_f + \left(-\frac{i}{n\pi} - 4i n \pi \zeta_f \right) \xi_{liq} + \left(10\zeta_f + \frac{n^2(-10\pi^3\zeta_f + 20\pi^3\zeta_f^2)}{15\pi} \right) \xi_{liq}^2 + \right. \\
& \quad \left(1 - \frac{4}{3} n^2 \pi^2 (3\zeta_e + \zeta_f) + \left(\frac{4i}{n\pi} + \frac{4}{3} i n^3 \pi^3 \zeta_e (-1+2\zeta_f) + 8i n \pi (3\zeta_e + 2\zeta_f) \right) \xi_{liq} \right) \mu_e + \\
& \quad \left. \left(-10 + \frac{1}{3} n^4 \pi^4 \zeta_e (-2+3\zeta_e + 2\zeta_f) - \frac{10}{3} n^2 \pi^2 (9\zeta_e + \zeta_f) \right) \mu_e^2 \right) \mu_f^3 + \\
& \left(1 + \frac{4}{3} n^2 \pi^2 \zeta_f + \left(\frac{i}{n\pi} + 10i n \pi \zeta_f + \frac{n^2(-5i n \pi^4 \zeta_f + 10\pi^4 \zeta_f^2)}{15\pi} \right) \xi_{liq} + \left(5 - \frac{1}{3} n^4 \pi^4 \zeta_e (-1+2\zeta_f) - \frac{10}{3} n^2 \pi^2 (3\zeta_e + 2\zeta_f) \right) \mu_e \right) \mu_f^4 + \\
& \left(1 - \frac{10}{3} n^2 \pi^2 \zeta_f - \frac{1}{15} n^4 \pi^4 (-1+2\zeta_f) \right) \mu_f^5
\end{aligned}$$

Eq. 39

6 Glossary

Variable	Definition	Comment
$\langle \rangle$	Area-average	
A	(Effective) area of the resonator plate	
C	Mass-sensitivity constant	Eq. 3
d	Thickness of a layer	
d_q	Thickness of the resonator	$d_q = m_q/\rho_q = Z_q/(2\rho_q f_0)$
D	Dissipation factor	$D = 1/Q = 2\Gamma/f_r$
e	As an index: electrode	Section 5.5
f	As an index: film	Section 5.5
f	Frequency	
\tilde{f}	Complex resonance frequency	$\tilde{f} = f_r + i\Gamma$
f_r	Resonance frequency also: “series resonance frequency”	Here: the undamped res. frequency
f_0	Resonance frequency at the fundamental	$f_0 = Z_q/(2m_q) = Z_q/(2\rho_q d_q)$
f_{os}	Oscillator strength	A number, not a frequency, Eq. 18
$g(\omega_{P,0})$	Weight function	Eq. 23
\tilde{G}	Shear modulus	
G_q	Shear modulus of AT-cut quartz	$G_q = 29 \times 10^9$ Pa, often called μ_q in the literature. Section 5.2, “ h ” for “height”
h_r	Characteristic vertical scale of roughness	
\tilde{J}	Shear compliance	
\tilde{k}	Wavenumber	$\tilde{k} = \omega/\tilde{c}$
liq	As an index: liquid	
l_r	Characteristic lateral scale of roughness	Eq. 12 and Eq. 13, “ l ” for “lateral”
L	Thickness of rough layer	Eq. 14 (roughness modeled by Darcy flow)
M_p	Mass of a particle	Eq. 18
m	Mass per unit area	
m_q	Mass per unit area of the resonator	$m_q = \rho_q d_q = Z_q/(2f_0)$
n	Overtone order	
N_p	Number of particles per unit area	Eq. 18
q	As an index: quartz resonator	
Q	Q-factor	$Q = 1/D = f_r/(2\Gamma)$
ref	As an index: reference state of a crystal in the absence of a load Or: reference frequency (Eq. 7)	
\hat{v}	Amplitude of tangential velocity	Eq. 1
\tilde{Z}	Acoustic wave impedance	Mostly a shear-wave impedance $\tilde{Z} = \rho\tilde{c} = (\rho\tilde{G})^{1/2}$
\tilde{Z}_L	Load impedance	Eq. 1
Z_q	Acoustic shear-wave impedance of AT-cut quartz	$Z_q = 8.8 \cdot 10^6$ kg m ⁻² s ⁻¹
β', β''	Power law exponents	Eq. 7 (“PL exp” in QTM)
χ^2	Measure of the quality of a fit	Eq. 6
γ_p	Decay constant of a particle resonance	Eq. 20
Γ	Imaginary part of a resonance frequency	$\Gamma = \Delta f_r/2$
δ	Penetration depth of a shear wave	Newtonian liquids: $\delta = (2\eta_{liq}/(\rho_{liq}\omega))^{1/2}$
δ_L	Loss angle	$\tan \delta_L = G''/G' = J''/J'$ often called δ in rheology
Δ	As a prefix: A shift induced by the sample	
$\tilde{\eta}$	Viscosity	$\tilde{\eta} = \tilde{G}/(i\omega)$
κ_p	Tangential spring constant	

μ	Non-dimensional mass	Eq. 24
ρ	Density	
ρ_q	Density of crystalline quartz	$\rho_q = 2.65 \text{ g/cm}^3$
$\hat{\sigma}_{ }$	Amplitude of tangential stress	Eq. 1
ξ_H	Cross section of effective pores ("permeability")	Eq. 14
ξ_{liq}	Non-dimensional shear-wave impedance of the bulk liquid	Eq. 24
ω	Angular frequency	
$\omega_{P,0}$	Undamped particle resonance frequency	Eq. 18
ζ	Non-dimensional inverse square shear-wave impedance	Eq. 24

7 References

- Johannsmann, D., Studies of Viscoelasticity with the QCM. In *Piezoelectric Sensors* Steinem, C.; Janshoff, A., Eds. Springer: Heidelberg, 2006.
- Johannsmann, D., Viscoelastic, mechanical, and dielectric measurements on complex samples with the quartz crystal microbalance. *Physical Chemistry Chemical Physics* **2008**, 10, (31), 4516-4534.
- Johannsmann, D. *The Quartz Crystal Microbalance in Soft Matter Research: Fundamentals and Modeling*; Springer, 2014.
- Steinem, C.; Janshoff, A. (eds.), *Piezoelectric Sensors* Springer: Heidelberg, 2007.
- Arnau, A. (edt.), *Piezoelectric Transducers and Applications*. Springer: Heidelberg, 2004.
- Cooper, M.A.; Singleton, V.T., A survey of the 2001 to 2005 quartz crystal microbalance biosensor literature: applications of acoustic physics to the analysis of biomolecular interactions. *Journal of Molecular Recognition* **2007**, 20, (3), 154-184.
- Becker, B.; Cooper, M.A., A survey of the 2006-2009 quartz crystal microbalance biosensor literature. *Journal of Molecular Recognition* **2011**, 24, (5), 754-787.
- Speight, R.E.; Cooper, M.A., A Survey of the 2010 Quartz Crystal Microbalance Literature. *Journal of Molecular Recognition* **2012**, 25, (9), 451-473.
- Daikhin, L.; Gileadi, E.; Katz, G.; Tsionsky, V.; Urbakh, M.; Zagidulin, D. Influence of roughness on the admittance of the quartz crystal microbalance immersed in liquids. *Anal. Chem.* **2002**, 74, 554-561.
- Dybwad, G. L. A Sensitive New Method for the Determination of Adhesive Bonding between a Particle and a Substrate. *J. Appl. Phys.* **1985**, 58, 2789-2790.
- Johannsmann, D. Towards vibrational spectroscopy on surface-attached colloids performed with a quartz crystal microbalance. *Sensing and Bio-Sensing Research* **2016**, 11, 86-93.
- Gillissen JJJ, Tabaei SR, Jackman JA, Cho NJ. A model derived from hydrodynamic simulations for extracting the size of spherical particles from the quartz crystal microbalance. *Analyst* **2017**, 3370-3379.
- Press, W. H.; Teukolsky, S. A.; Vetterling, W. T.; Flannery, B. P., *Numerical Recipes: The Art of Scientific Computing*. 3 ed.; Cambridge University Press: 2007.
- Fritze, H.; Tuller, H. L. Langasite for high-temperature bulk acoustic wave applications. *Appl. Phys. Lett.* **2001**, 78, 976-977.
- Sievers, P. Moß, C., Schröder U., Johannsmann. D. *Use of Torsional Resonators to Monitor Electroactive Biofilms*, in preparation
- Johannsmann, D., Viscoelastic analysis of organic thin films on quartz resonators. *Macromolecular Chemistry and Physics* **1999**, 200, (3), 501-516.
- Voinova, M. V.; Jonson, M.; Kasemo, B. 'Missing mass' effect in biosensor's QCM applications. *Biosens. Bioelectron.* **2002**, 17, 835-841.